CLM - P 222

This document is intended for publication in a journal, and is made available on the understanding that extracts or references will not be published prior to publication of the original, without the consent of the authors.

CULHAM LABORATORY

ABINGDON OXFORDSHIRE

United Kingdom Atomic Energy Authority

RESEARCH GROUP

Preprint

STUDY OF TURBULENCE WITHIN A COLLISIONLESS SHOCK USING COLLECTIVE SCATTERING OF LIGHT

J. W. M. PAUL
C. C. DAUGHNEY
L. S. HOLMES

Culham Laboratory
Abingdon Berkshire

1969

Enquiries about copyright and reproduction should be addressed to the
Librarian, UKAEA, Culham Laboratory, Abingdon, Berkshire, England

CLM - P 222

STUDY OF TURBULENCE WITHIN A COLLISIONLESS SHOCK USING COLLECTIVE SCATTERING OF LIGHT

by

J.W.M. PAUL
C.C. DAUGHNEY
L.S. HOLMES

(To be published in the Proceedings of the ESRIN Study Group on Collision-free Shocks in the Laboratory and Space, Frascati, June 1969)

A B S T R A C T

The currently accepted theories of collisionless shocks with low Alfven Mach number, invoke ion wave turbulence to explain the resistive heating and the shock structure. These ion waves have fluctuating electric fields which scatter and consequently heat electrons, and also have fluctuating electron densities which can scatter light. This latter process has been used to study the turbulence within these shocks.

We present measurements of a supra-thermal level of ion wave fluctuations within the shock. From this we have estimated the energy in the turbulence and the effective collision frequency. The latter is sufficient to explain the observed shock heating.

We also present recent measurements of the spectral profiles of the light scattered by these ion waves. The profiles demonstrate that the ion waves propagate in the direction of the electron current with the ion wave phase velocity but are heavily damped. This damping results in many random changes of phase during an effective collision time.

U.K.A.E.A. Research Group,
Culham Laboratory,
Abingdon, Berks.

October, 1969 (SLW)

C O N T E N T S

PART 1 : INTRODUCTION

1.1. Shock Experiment*

We have previously described a collisionless shock with low Alfven Mach number ($M_A < 3$), which propagates perpendicular to a magnetic field[1,2,3]. The shock is produced by the radial compression of an initial hydrogen plasma within a linear Z-pinch. The initial plasma is 85% ionized with electron density $n_{e1} = 6{\cdot}4 \times 10^{20} m^{-3}$, and temperatures $T_{e1} = T_{i1} = 1{\cdot}2$ eV, and is in an axial magnetic field $B_{z1} = 0{\cdot}12$ Wb m^{-2}. The shock propagates radially inwards through the initial plasma with a steady velocity $V_s = 240$ km s^{-1} ($M_A = 2{\cdot}5$), and with a steady structure of width $L_s = 1{\cdot}4$ mm, rise time 6 ns and compression ratio $F = 2{\cdot}5$. The measured electron temperature behind the shock, $T_{e2} = 44$ eV, implies a resistivity within the shock which is about two orders of magnitude greater than the classical collisional value[4]. This demonstrates the collisionless nature of the shock.

An effective mean resistivity ($\bar{\eta}$), can be estimated from a simplified resistive power balance equation,

$$\bar{\eta}(F-1)^2\left(\frac{B_{z1}}{\mu_o L_s}\right)^2 L_s = (n_{e1}\, V_s)\; 1{\cdot}5\; \kappa\; (T_{e2} - T_{e1}) \quad \text{(M.K.S.)}$$

The result corresponds to a collision frequency,

$$\bar{\upsilon} = 3 \times 10^9 \text{ Hz}$$

A "collisionless" process is required to explain this suprathermal collision frequency.

The mean electron drift velocity (v_d) within the shock is

---

* See earlier lecture at this conference, "Review of Experimental Studies of Collisionless Shocks Propagating Perpendicular to a Magnetic Field" By J.W.M. Paul.

about four times the ion sound speed (c_s) and a tenth of electron thermal velocity (v_e). For these conditions,

$$c_s < v_d < v_e \quad \text{and} \quad T_e > T_i$$

the best available theories[5-8] predict that the current driven ion wave instability should occur. The non-linear phase of this instability[9] will lead to a supra-thermal level of fluctuation (i.e. turbulence) with $\lambda > \lambda_D$, the Debye length and $\omega \lesssim \omega_{pi}$.

The fluctuating electric fields in this turbulence will produce an effective collision frequency and stochastic heating of particles provided there is sufficient randomness of phase. The fluctuating density in the tubulence will give enhanced scattering of light. This light scattering has proved a most powerful demonstration and diagnostic of this turbulence.

1.2. Scattering Theory

When light is scattered by plasma waves[10-12], the change of optical wave vector and frequency are related to the plasma wave vector ($\bar{k}$) and frequency (ω) by the equations of conservation of momentum and energy

$$\bar{k}_s = \bar{k}_i \pm \bar{k} \quad ; \quad \omega_s = \omega_i \pm \omega$$

where the subscript s is for scattered and i for incident. The positive and negative signs correspond to plasma waves propagating in opposite directions.

For small change in the incident wavelength λ_i (i.e. $|k_i| = |k_s|$), $|\bar{k}|$ is given by the scattering angle θ as follows,

$$|k| = |k_s - k_i| = \frac{4\pi}{\lambda_i} \sin\left(\frac{\theta}{2}\right),$$

while the frequency spectrum of the waves with this $|k|$ and

$\bar{k} = \pm (\bar{k}_s - \bar{k}_i)$ is given by the spectral profile, $\Delta\lambda = \lambda_s - \lambda_i$, of the scattered light

$$\omega = \pm (\omega_s - \omega_i) = \mp \left(\frac{2\pi c}{\lambda_i^2}\right) \Delta\lambda$$

Opposite wavelength shifts ($\pm \Delta\lambda$) correspond, through the sign of $\bar{k}$, to waves propagating in opposite directions. The same conclusions can be obtained by considering the doppler shift of light scattered from the moving pattern of the waves.

The fraction of the power scattered into solid angle $d\Omega$ per unit length of laser beam is given by

$$dP = n_e \sigma (\omega, \bar{k})\, d\Omega\, d\omega .$$

The differential scattering cross-section per electron, $\sigma(\omega, \bar{k})$, measures the level of density fluctuation in terms of its Fourier transform,

$$\sigma(\omega, k) = \frac{\langle \delta n_e^2(\omega, k) \rangle}{n_e} \sigma_e = S(\omega, k)\sigma_e ,$$

where σ_e is the appropriate Thomson scattering cross section for a single electron and

$$\langle \delta n_e^2(\omega, \bar{k}) \rangle = \iint \langle \delta n_e^2(\bar{r}, t) \rangle \exp[-i(\bar{k} \cdot \bar{r} + \omega t)] d\bar{r}\, dt.$$

In the absence of spectral resolution, the cross-section measures

$$S(k) = \int S(\omega, k)\, d\omega .$$

For the plasma conditions within the shock, as described in Section 1.1, and for incident ruby laser light, scattering from plasma waves ($k \leqslant 1/\lambda_D$) can be observed only for small scattering angles ($\theta \lesssim 5^o$), i.e. forward scattering.

1.3. Scattering Experiment

We have studied[3,13,14] the light forward-scattered from a 50 MW ruby laser beam of diameter 2 mm, during the passage of the shock through the beam. The experimental arrangement is shown in

Fig.1. The laser pulse width of 35 ns is greater than the transit time of the shock through the laser beam (10 ns). The timing of the shock relative to the laser pulse is obtained from the shock luminosity or from an electric probe which is azimuthally out of the optical paths. The incident and forward-scattered light paths intersect symmetically in the midplane of the discharge tube at an angle of $5{\cdot}1^{o}$ (see footnote*). Both light paths are in a plane which is tangential to the shock front when at 9 cm radius.

The plasma waves responsible for this scattering have a mean wave vector $\bar{k}$ lying within a double cone of half angle 12^{o} with its axis colinear with the azimuthal current within the shock. The magnitude of $\bar{k}$ lies within the range[/] $|\bar{k}| = k_m = 8{\cdot}2 \pm 2{\cdot}1 \times 10^5\ m^{-1}$. The nature of the plasma waves depends on the parameter $\alpha = 1/(k\lambda_D)$, where λ_D is the Debye distance. For this experiment, α varies in the range $3{\cdot}8 > \alpha > 1{\cdot}0$ between the front and rear of the shock respectively, with $\alpha = 1{\cdot}1$ for the mean conditions.

The laser power incident on the plasma is monitored by a photodiode. This signal is used to obtain the ratio of scattered to incident power, the "normalized scattered power".

PART 2 : MAIN EXPERIMENTS

2.1. Enhanced Scattering

The scattered light, measured by a photomultiplier, appears as a pulse, shown in Figs.2 and 3, which is much shorter than the laser emission, and corresponds in time and duration with the passage of

---

* A recent measurement revealed that this angle is not $4{\cdot}5^{o}$ as was reported previously.

/ As a result of the new value for θ, k_m has changed from the previously reported[3,14] value of $7{\cdot}1 \times 10^5\ m^{-1}$.

the shock through the laser beam. The rise time of the pulse (5 ns) is just within the limit of the photomultiplier response.

In these measurements the scattered power from the shock is superimposed on a 6% spurious background signal. This background is observed even when the detecting system does not view the laser beam, but only when the pre-ionization discharge has occurred. As the background persists long after the plasma has gone, it is attributed to electrode material. Unfortunately this spurious signal prevents measurements of the scattering from the pre- or post-shock plasma. With more gain in the detecting system the short pulse of enhanced forward scattering from the shock can be seen above the spurious background even when it occurs late or early in the laser pulse (Fig.3). Such measurements show that the normalised scattered power is independent of laser power for over an order of magnitude variation of the latter.

Although there is no space or time resolution within the shock, there is clearly an enhanced level of scattering and consequently an enhanced level of fluctuation at $k = k_m$ within the shock.

We have also measured light which is back-scattered through 170^o ($\alpha \ll 1$). Spectral resolution of this back-scattered light is obtained by using a wide pass-band (30 Å) filter set at about 50 Å off the ruby line so that a signal appears only when the electrons are appreciably heated. As shown in Fig.3., this back-scatter signal is insignificant from the cold initial plasma, but appreciable from the hot post-shock plasma. These measurements demonstrate that the electron heating is coincident with the burst of enhanced forward scattering.

2.2. Presence of Ion Waves

Spectral resolution of the forward scattered light is obtained by either (i) interference filters with 3 Å or 35 Å pass band centred on the laser line, or (ii) a 3 Å filter in front of a Fabry-Perot interferometer as shown in Fig.1. The interferometer is temperature controlled to $\pm 0{\cdot}1^{\circ}C$, and is scanned by varying the refractive index (pressure) of the gas between the plates.

The measured normalised scattered power within the 3 Å and 35 Å pass bands is the same within the experimental accuracy (± 15%). Thus the scattering produces a change of wavelength $\Delta\lambda < 1{\cdot}5$ Å and must arise from plasma fluctuations with frequencies appreciably less than the electron plasma frequency, for which $\Delta\lambda = 5$ Å. As there is no reason to expect appreciable Doppler-shifting of the plasma frequency, this result excludes the possibility of an enhanced level of electron plasma waves*.

In the first measurements with the Fabry-Perot interferometer, the free spectral range was 3 Å, to overlap with the 3 Å filter. The corresponding resolution was 0·08 Å. The spectral profiles obtained from the Fabry-Perot interferometer are normalised by using a photomultiplier and glass-plate splitter to monitor the scattered power incident on the interferometer. These measurements demonstrate that all the scattered light lies within the wavelength range ± 0·15 Å from the centre of the ruby line, as shown in Fig.4. The spectral half width $\Delta\lambda = 0{\cdot}075$ Å, which is about twice that of the incident light, is equivalent to a frequency change $\Delta\omega = 3 \times 10^{10}$ Hz. This corresponds to scattering from plasma waves with

---

* See earlier lecture at this conference, "Review of Experimental Studies of Collisionless Shocks Propagating Perpendicular to a Magnetic Field" By J.W.M. Paul.

$$\omega = \Delta\omega < \omega_{pi}$$

where the ion plasma frequency $\omega_{pi} = 5 \times 10^{10}$ Hz. Although the structure of the spectral profile $S(\omega, k_m)$ is not resolved, these measurements provide evidence that the enhanced fluctuations within the shock are ion waves.

2.3. Measurement of Scattering Cross-Section

The average scattering cross-section within the shock has been measured by comparing the power scattered from the shock, with that Rayleigh-scattered[15] from nitrogen gas. This method of calibration has been checked by showing that the normalised power scattered from nitrogen is proportional to gas pressure and independent of laser power, while giving the correct ratio to the scattering from neon gas to within 10%. An independent, but less accurate, calibration of the laser power, using a calorimeter, and of photomultiplier sensitivity against a thermo pile, agreed to within 30% with that obtained from the Rayleigh scattering.

The ratio (R) of the scattered power from the shock to that from nitrogen gas, with number density n_n, is given by

$$R = G\left(\frac{n_e\,\sigma(k_m)}{n_n\,\sigma_R}\right) = \left(\frac{G}{n_n\,\sigma_R}\right)\langle\delta n_e^2(k_m)\rangle = G\cdot\left(\frac{n_e}{n_n}\frac{\sigma_e}{\sigma_R}\right)S(k_m)$$

where σ_R is the Rayleigh cross-section for nitrogen and G is a geometrical factor ($G = 2{\cdot}3$) arising from the different scattering volumes of the shock and the nitrogen.

The measured ratio of scattered power from the shock to that from nitrogen gas yields a level of fluctuation within the shock,

$$\langle\delta n_e^2(k_m)\rangle = 4{\cdot}2 \times 10^{23}\ m^{-3}\ .$$

This corresponds to,

$$\sigma(k_m) = 3{\cdot}3 \times 10^{27} \quad \text{and} \quad S(k_m) = 430 ,$$

for the mean value of n_e within the shock, while for the limiting values at the front and rear,

$$780 > S(k_m) > 290$$

respectively. The same level of fluctuation is measured with and without the electric probe in the plasma. The standard deviation of these measurements is 15%, but some records vary by as much as a factor of two.

It is interesting to note that this enhancement is not observed for the higher Mach number shock ($M_A = 3{\cdot}7$) reported previously[1,2,3].

PART 3 : COMPARISON OF RESULTS WITH THEORY*

3.1. Ion Wave Turbulence

For a stable homogeneous unmagnetised plasma with no current, scattering theory[10,11] states that $S(k) \leqslant 1{\cdot}0$. The presence of a uniform current, unless very close to instability, does not appreciably alter this result[12] nor does the presence of a homogeneous magnetic field.

The high value of $S(k_m)$ observed in this experiment implies the presence of instability and subsequent non-linear limitation. The free energy driving this instability must be associated with the current flow or the inhomogeneities within the shock. In this resistive shock, these are interdependent and although no complete theory exists, ion wave turbulence is predicted[6-8]. These predictions are verified by the experimental results. The two main

---

* See earlier lecture at this conference, "Review of Experimental Studies of Collisionless Shocks Propagating Perpendicular to a Magnetic Field" By J.W.M. Paul.

theoretical approaches to the ion wave instability problem will be discussed in the next two Sections.

3.2. Homogeneous Plasma Theory of Kadomtsev

A non-linear theory of homogeneous ion wave turbulence in the absence of a magnetic field has been developed by Kadomtsev[9]. He balances a constant linear growth rate against non-linear scattering of the waves on ion. This scattering removes energy from the unstable region at high $k(\sim 1/\lambda_D)$ and diffuses it towards an infinite sink at $k = 0$. The balancing process results in a spectrum of turbulence*

$$\langle E^2(k)\rangle = \frac{(2\pi)^3}{7}\left(\frac{V_d}{V_e}\right)\left(\frac{T_e}{T_i}\right)\frac{1}{\psi^2}\frac{(\kappa T_e)^2}{4\pi e^2}\frac{1}{k}\ln\left(\frac{1}{k\lambda_D}\right)$$

spread over a single conical region of $\bar{k}$ (Cerenkov cone for emission of phonons) with axis directed along $\bar{v}_d$ and half angle $\psi = \cos^{-1}(c_s/v_d)$.

The relation between the predicted $\langle E^2(k)\rangle$ and the observed $\langle \delta n_e^2(k)\rangle$ can be obtained by assuming that the linear dispersion relations[16] for ion waves hold within the shock. The relations for an unmagnetized plasma are used on the grounds that $\omega_{ci} \ll \omega_{pi}$, $\omega_{ce}\cos\varphi \ll \omega_{pi}$ ($90^o - \varphi$ is the angle between $\bar{k}$ and $\bar{B}$) and Bernstein modes should not be important. The dispersion relations yield

$$\frac{\langle E^2(k)\rangle}{k^2} = \left(\frac{m_e}{e}\right)^2 \frac{c_e^4}{n_e^2}\langle \delta n_e^2(k)\rangle$$

where

$$c_e^2 = (\gamma_c\, \kappa T_e/m_e)$$

For the mean shock conditions, $v_d/v_e = 0{\cdot}1$, $T_i = 1{\cdot}7$ eV for

---

* This formula was taken from ref(9) p.71 by combining $E_k^2 = k^2 I_k$ and the formula for I_k. The factor $(2\pi)^3$ appears from converting the Fourier transform to the form used in light scattering theories.

adiabatic heating with $\gamma_i = 5/3$, $c_e = v_e$ for isothermal electrons ($\gamma_e = 1$), and $\psi \approx \pi/2$ for $v_d \gg c_s$. The above formulae then yields

$$\langle \delta n_e^2(k_m) \rangle = 8 \times 10^{23} \ m^{-3} \ .$$

Thus the Kadomtsev theory predicts a fluctuation level for the mean shock conditions which is about twice that observed.

3.3. Inhomogeneous Plasma Theory of Krall*

This theory[7,8] considers the more realistic conditions of plasma flow through a magnetic shock front. Electron drift motions due to ∇B, ∇n and $E \times B$ are included. The stability of waves propagating in the (r, θ) plane (i.e. perpendicular to B) is considered. The resonance of these waves with the electron drift results in ion wave instability. As a consequence of the plasma flow, the unstable waves have both k_r and k_θ components. Linear instability theory yields a maximum growth rate $\gamma = \sqrt{\omega_{ce}\, \omega_{ci}}$ in the region

$$\left[\frac{1}{2r_{ce}}\right] < |k| < \frac{1}{\lambda_D}$$

and with $k_\theta \ll k_r$ ⁄. This theory contains no diffusion terms and so there should be no appreciable enhancement at $k_\theta \sim 1/\lambda_D$. This is in conflict with the observations reported here.

PART 4 : ESTIMATE OF THE ENERGY IN TURBULENCE

The total energy in the turbulence, assuming that it is isotropic‡, can be estimated from the measured level of fluctuation. The linear ion wave dispersion relations, mentioned above, are assumed

---

* See contribution to this conference by N. Krall

⁄ According to discussion during the conference, the parameters of most experiments yield, $k_\theta \sim 1/r_{ce}$ spread over a range of k_r from $1/r_{ce}$ to $1/\lambda_D$.

‡ The latest results, given in Section 6, show that this assumption is not true.

and used to obtain the relations[16] between the three forms of potential energy $\langle \delta n_e^2(k) \rangle$, $\langle \delta n_i^2(k) \rangle$ and $\langle E^2(k) \rangle$ in the waves for a given k value. The ratio of the total energy, $W_T(k)$ to that in the electron density fluctuations, $W_n(k)$, at a given k can be expressed

$$\frac{W_T(k)}{W_n(k)} = 2(1+X^2)(1+t+X^2) = F(X, t) \quad *$$

where $X = k\lambda_D$ and $t = T_e/T_i$. While

$$W_n(k) = W_e \frac{S(k)}{n_e}$$

where $W_e = \frac{1}{2} m_e n_e v_e^2$, the electron kinetic energy density ($\gamma_e = 1$). The total energy integrated over the spectrum

$$W = \frac{1}{2\pi^2} \int_0^{k_{max}} W_T(k) \, d^3k$$

The turbulent spectrum can be expressed in dimensionless form by normalizing to the value at $k = k_m$.

$$\langle E^2(k) \rangle = \Gamma(k, k_m) \langle E^2(k_m) \rangle$$

so that

$$S(k) = \Gamma(k, k_m)(k_m/k)^2 S(k_m)$$

Combining the above equations, the ratio of the total energy in the ion wave turbulence to the electron thermal energy

$$Q = \frac{W}{W_e} = \frac{2}{3\pi} \frac{S(k_m)}{N_D} J(k_m, k_{max})$$

where $N_D = (4/3)\pi\lambda_D^3$ and

$$J(k, k_{max}) = X_m^2 \int_0^{X_{max}} \Gamma(X, X_{max}) F(X, t) dX$$

---

* There are limitations on the validity of this equation, see reference 17.

We further assume that the k-spectrum of the turbulence has the form of a power law, $\Gamma(k , k_m) = (k/k_m)^N$. Integration shows that Q is finite only for $N \geqslant -1$. The limiting value $N = -1$, which corresponds to the Kadomtsev spectrum, yields the maximum value of Q, which for the mean shock conditions is about 12%. Thus, on the basis of these assumptions, for which we offer no proof, we have obtained a limiting estimate of the energy in the turbulence. This estimate suggest that neglect of this energy in the fluid equations is justified.

PART 5 : ESTIMATE OF THE EFFECTIVE COLLISION FREQUENCY

5.1. Stochastic Approach

There are two different approaches, quasi-linear and stochastic, to estimating the effective collision frequency in a turbulent plasma. Also, for each method there are two different frequencies corresponding to momentum and energy transfer:

(1) Quasi-linear estimates of $v\ \partial f/\partial t$ and $v^2\ \partial f/\partial t$ yield collision frequencies for momentum and energy transfer respectively.

(2) Stochastic calculations use the Fokker-Planck equation[18]. The perpendicular diffusion coefficient and the dynamical friction coefficient correspond to momentum and energy transfer respectively.

In the following we shall adopt the stochastic approach[19] as the simpler. We consider a test particle with initial velocity $\bar{u}_o$. We shall later identify this velocity with the random thermal velocity of the electrons. The test particle experiences interactions with an isotropic* fluctuating field $\langle E^2(\omega , k)\rangle$. Resistivity is usually

---

* The latest results given in Section 6, show that this assumption is not true.

defined by a momentum balance, so we shall estimate the momentum transfer collision frequency.

The stochastic deflections experienced by the test particle (electron) in the fluctuating electric field eventually result in a total deflection of 90^{o}, i.e. an effective binary collision. The time for such a collision can be defined as the time after which the average square of the velocity perpendicular to $\bar{u}_o$ equals u_o^2

$$\langle u_\perp^2 \rangle = u_o^2$$

Thus the effective collision frequency is given by

$$\nu^* = \frac{1}{u_o^2} \frac{\partial \langle u_\perp^2 \rangle}{\partial t} \Bigg|_{t=0}$$

This sideway diffusion of the particle can be related to the Fokker-Planck velocity-space diffusion coefficient $(D_\perp)$

$$D_\perp = \frac{\partial \langle u_\perp^2 \rangle}{\partial t} \Bigg|_{t=0}$$

This perpendicular diffusion coefficient has been evaluated for a fluctuating electric field by Thompson and Hubbard[20] and described also by Sitenko[18] and Sturrock[21].

$$D_\perp = \frac{1}{(2\pi)^3} \left(\frac{e}{m} \right)^2 \int \left(1 - \frac{(\bar{k} \cdot \bar{u}_o)^2}{k^2 u_o^2} \right) \langle E^2(\omega, k) \rangle \delta(\omega + \bar{k} \cdot \bar{v}) d^3k d\omega$$

where

$$\langle E^2(\omega, k) \rangle = \int \langle E^2(\bar{r}, t) \rangle \exp\left\{ -i(\bar{k} \cdot \bar{r} + \omega t) \right\} d\bar{r}\, dt$$

For our purposes this diffusion coefficient, involving an integration over all waves for a single test particle, should also be evaluated for all u_o in the Maxwellian velocity distribution and again integrated.

5.2. Simplifications

We have made the following simplifications in order to evaluate $D_\perp$:

(i) The waves are ion waves for which the phase velocity (c_s) is much less than the mean electron thermal velocity (v_e). For $v_e \gg c_s$ the electrons effectively experience a time independent wave spectrum, i.e.

$$\langle E^2(\omega, k)\rangle \approx \langle E^2(k)\rangle\, \delta(\omega)$$

The reasonance term $\delta(\omega + \bar{k} \cdot \bar{u}_o)$, when combined with the above $\delta(\omega)$, yields $\delta(\bar{k} \cdot \bar{u}_o)$, i.e. $|\bar{k} \cdot \bar{u}_o| = \omega \approx 0$. The resonances occur for particles and waves moving almost perpendicular to each other. The few slow particles at other angles are neglected.

(ii) As $\bar{k} \cdot \bar{u}_o = 0$ for the particles and waves of interest, the first bracket under the integral reduces to unity*. A further simplification is obtained by substituting the relation

$$\delta(\bar{k} \cdot \bar{u}_o) = \frac{1}{|u_o|}\, \delta(k_\parallel)$$

(iii) If we assume that the wave spectrum is isotropic we can put $d^3k = 2\pi k_\perp dk_\perp dk_\parallel$ and integrating over $k_\parallel$,

$$D_\perp = \frac{1}{(2\pi)^2}\left(\frac{e}{m_e}\right)^2 \frac{1}{|u_o|} \int_0^{k_{max}} \langle E^2(k_\perp)\rangle k_\perp dk_\perp$$

Now we can simply drop the $\perp$ subscript.

---

* In references (3,14) a mean value of $\bar{k} \cdot \bar{u}$ was taken, and this made the bracket 2/3.

(iv). We assume that, as $v_d \ll v_e$, the electron distribution function is also isotropic. The effective collision frequency can be obtained by suitable integration over a Maxwellian distribution of test particles, i.e. values of $|u_o|$. As $v_e \gg c_s$ and we have already assumed $\bar{k} \cdot \bar{u}_o = 0$, we can approximate the distribution of $|u_o|$ by using the mean electron thermal velocity v_e in $D_\perp$.

With these simplifications, for which we offer no proof, we obtain

$$\nu^* = \frac{1}{u_o^2} D_\perp \approx \frac{1}{4\pi^2} \left(\frac{e}{m} \right)^2 \frac{1}{v_e^3} \int_0^{k_{max}} \langle E^2(k) \rangle k dk \ .$$

5.3. Evaluation

The integration limit k_{max} is assumed to correspond to the cut-off of collective effects for $k > 1/\lambda_D$. Stringer[5] and Krall[7,8] have shown that appreciable linear growth for this instability occurs for $k < 1/\lambda_D$. Thus $k_{max} = (1/\lambda_D)$.

The turbulent spectrum $\langle E^2(k) \rangle$ can be represented by $\langle \Gamma(k, k_m) \rangle$ as in Section 4, and converted to $\langle \delta n_e^2(k) \rangle$ as in Section 3.2. The effective collision frequency can now be put in the form

$$\nu^* = \frac{1}{3\pi} \frac{\omega_{pe}}{N_D} S(k_m) I(k_m)$$

where

$$I(k_m) = X_m^2 \int_0^1 \Gamma(X, X_m) X dX$$

and $X = k\lambda_D$.

We now assume that the spectrum can be represented by a power law $\Gamma(k, k_m) = (k/k_m)^N$, as in Section 4, with $N \geq -1$ for finite

energy. Integration yields

$$I(k_m) = \frac{X_m^{2-m}}{N+2} = \frac{(k_m\lambda_D)^{2-N}}{N+2}$$

If the integration limit k_{max} is left in, it is clear that the value of ν^* depends mainly on the part of the spectrum near k_{max}, which for this case is $1/\lambda_D$.

We next assume that the enhanced scattering occurs for the mean or rear plasma conditions ($\alpha \sim 1$) rather than the initial conditions ($\alpha \sim 4$). Then our measured enhancement at k_m is at the dominant part of the spectrum and the exact form of the spectrum is less important.

We have assumed $N = -1$, corresponding to the Kadomtsev spectrum, and evaluated the effective collision frequency. For the mean shock conditions

$$\nu^* = 1{\cdot}0 \times 10^{10}\,\text{Hz}\ \not$$

Even if the power law is changed to $N = +2$, ν^* is only halved. The limiting values of ν^* for conditions at the front and rear of the shock with $N = -1$ are

$$22\ \text{GHz} > \nu^* > 5\ \text{GHz}$$

respectively.

The collision frequency for the mean shock conditions, is about three times that ($\bar{\nu}$) estimated more directly through the resistivity in Section 1.1. Consequently the measured level of fluctuation within the shock, (with the above assumptions), is sufficient to explain the observed electron heating. Within the accuracy of the estimates of $\bar{\nu}$ and ν^*, we have obtained experimental evidence for a self-consistent model of a collisionless shock based on ion-wave turbulence.

$\not$ This is larger than the previously reported[14] value, $\nu^* = 4{\cdot}5$ GHz, because of the two corrections, firstly on θ and secondly on $D_\perp$.

PART 6 : RECENT RESULTS

6.1. Measurement of the Spectral Profile $S(\omega, k_m)$ for $\pm B_{Z1}$

Recent measurements of the spectral profile of the scattered light have been obtained after two main changes in the system. Firstly, the spectral resolution of the Faby-Perot interferometer was changed to 0·02 Å by reducing the free spectral range to 0·75 Å. The stability of the interferometer to absolute drift of the fringe system was also improved. Secondly, the spectral width of the incident laser line was reduced to a measured value of 0·03 Å corresponding to 0·02 Å after correction for the instrumental width. This narrow line was achieved by modifying the resonant reflector of the oscillator cavity. The single sapphire resonant reflector was replaced by a triple etalon reflector which was temperature controlled to ± 0·1°C. The laser emission contained two satellite lines of similar width but each with a third of the central intensity. These satellites at ± 0·43 Å from the central line were out of the spectral region of interest.

For measurements of the spectral profiles of both the incident laser light (from Rayleigh scattering) and the scattered light from the shock, the signal was normalized to the scattered power incident on the Fabry-Perot rather than to the incident laser power.

A spectral profile of the enhanced scattered light has been obtained with resoltuion of 0·02 Å for the same conditions as the previously described rough spectral profile with resolution 0·08 Å. Fig.5 shows the measured profile with error bars which are the standard deviations of about four measurements. The width of the profile at half intensity $\delta\lambda$ = 0·06 Å, is three times the width of the incident laser line.

The peak of the profile is shifted to the red by $\Delta\lambda = 0{\cdot}07$ Å from the laser line. This corresponds to scattering from plasma waves with frequency $\omega_0 = 28$ GHz. The shifted line has a full width at half intensity, $\delta\lambda = 0{\cdot}06$ Å which is comparable to this shift. The direction of the shift corresponds to the enhancement of waves propagating in the same direction as the azimuthal electron current in the shock front. This current arises from the compression of the initial axial magnetic field by the shock. The vector directions are shown in Fig.5. The direction of this azimuthal current in the shock front can be reversed simply by reversing the axial magnetic field. In a z-pinch, with orthogonal drive and initial magnetic field, such a reversal has no effect on the plasma behaviour other than to change the "hand". This would not be true for a θ-pinch.

Reversal of the azimuthal current in the shock is this way resulted in a reversal of the sign of the shift of wavelength of the scattered light as shown in Fig.5. Thus it is the waves propagating in the direction of the electron current which are enhanced. This demonstrates that the instability is driven by the electron current.

The smooth curves shown in Fig.5 are the best fit to the whole set of observations irrespective of the sign of the wavelength shift. The good fit of the experimental points to the smooth curve shows the symmetry of the reversal of sign with reversal of current. The profiles are also, within experimental error, symmetrical about the shifted peak at $\Delta\lambda = 0{\cdot}07$ Å. (Note that the S.D. of the mean points is about half that of the individual measurements as shown by the error bars).

6.2. Discussion

There is clearly an ion wave mode in the plasma. The frequency

ω_o = 28 GHz, is lower than, but comparable with, the ion plasma frequency within the shock, for which 35 GHz < ω_{pi} < 56 GHz between front and rear respectively, with ω_{pim} = 44 GHz for the mean conditions. Thus

$$\omega_o = 0{\cdot}64\ \omega_{pim}$$

This frequency ω_o and the mean shock $k_m\lambda_D$ fit reasonably well onto the ion wave dispersion curve for B = 0, γ_e = 1 (isothermal electrons) and $T_e > T_i$, i.e.

$$\left(\frac{\omega}{\omega_{pi}}\right)^2 = \frac{(k\lambda_D)^2}{1 + (k\lambda_D)^2}$$

as shown in Fig.6*.

The turbulence is clearly not isotropic. The difference of scattered power from waves with oppositely directed $\bar{k}$, is at least 50 for $\omega = \omega_o$. Effectively only the mode propagating with the electron drift is enhanced. The turbulence clearly reflects the driving source, the electron drift current.

This lack of isotropy will affect the estimated of energy in the turbulence made in Section 4, and the estimate of the effective collision frequency made in Section 5. Until the dependence of $\langle\delta^2 n_e(k)\rangle$ on direction is known, it is not possible to make any corrections to these estimates. However, if the turbulence is uniformly spread over a hemisphere in k space, as is assumed by Kadomtsev for $v_d \gg c_s$, then our previous estimates would need to be halved.

Asymmetric profiles of scattered light have been observed previously[10] but the results presented here provide the first clear shift and first identification of the electron drift as the cause of

---

* Measurements made immediately after the conference showed that ω_o was proportional to ω_{pi} for constant α within the shock.

the asymmetry. The spectral profiles are similar to those predicted by Rosenbluth and Rostocker[12] for a stable plasma with large electron drift and $T_e > T_i$ except that the observed line near ω_{pi} is much broader and the $S(\omega, k)$ much larger than predicted for a stable plasma.

The large width of the scattered spectrum is significant. We assume that although the spectrum was obtained from different shots, it represents the spectrum of a single shot. The spectral width of the line centred on ω_o then measures the damping of this mode. (It could not represent a steady growth as there would be forty exponentiation times during the shock transit). The possibility that the observed spectrum reflects a dependence on $k\lambda_D$, through the dispersion relations, rather than a dependence on ω is most unlikely. The argument is illustrated in Fig.5. The observed line is symmetrical about ω_o, which would not be expected for ω_o near ω_{pi} and a dependence on $k\lambda_D$. Also there is appreciable scattering for $\omega > \omega_{pi}$, which is difficult to explain using the assumed dispersion relations without an appreciable damping width.

The width of the line is comparable with its shift. This means that the damping time or lifetim (τ_ℓ) of the mode is comparable with the period,

$$\tau_\ell \sim \frac{2\pi}{\omega_o} = 2{\cdot}2 \times 10^{-10} \text{second}$$

The mode is very heavily damped but still exists. It has not degenerated into a Gaussian profile about $\omega = 0$ as would occur for $\tau_\ell \ll (1/\omega_o)$.

The lifetime of the mode represents the interval between random changes of phase as the waves grow and damp, that is the correlation time. This randomness of phase is an essential aspect of the

stochastic calculation in Section 5. We are now in a position to show that this random phase approximation is reasonable.

In Section 5 th stochastic problem was reduced to that of a test particle with velocity v_e interacting with a stationary electric field pattern. The randomness of phase arises from the spatial extent of the correlation of phase, that is the correlation length (ℓ). This is simply related to the lifetime, τ_ℓ, by the ion wave phase velocity (c_s).

$$\ell = c_s \tau_\ell$$

The test particle now experiences a random change of phase after a time

$$\tau = (\ell/v_e) = \tau_\ell(c_s/v_e)$$

For the mean shock conditions $\tau \sim 5 \times 10^{-12}$ second, so that in one effective collision time,

$$\tau_{col} = (1/\nu^*) \sim 3\times 10^{-10} \text{ s}$$

the test particle experiences about 60 random changes of phase.

ACKNOWLEDGEMENTS

We thank Drs R.J. Bickerton and I. Cook for their advice and Mr P.R.I. Hedley for his assistance.

REFERENCES

1. PAUL, J.W.M., HOLMES, L.S., PARKINSON, M.J. and SHEFFIELD, J. Nature, 208, 133, 1965; also 7th Int. Conf. Phen. in Ionized Gases, (Belgrade) II, 319, 1965.

2. PAUL, J.W.M., GOLDENBAUM, G.C., IIYOSHI, A., HOLMES, L.S., and HARDCASTLE, R.A., Nature, 216, 363, 1967.

3. PAUL, J.W.M. Contribution to "Physics of Hot Plasmas", Scottish Universities 9th Summer School, 1968, Oliver and Boyd, Edinburgh.

4. SPITZER, L., and HÄRM, R. Phys. Rev., 89, 977, 1953.

5. STRINGER, T.E., J. Nucl. Energy, C. 6, 267, 1964.

6. SAGDEEV, R.Z. Rev. of Plasma Physics, 4, 23, 1966.

7. KRALL, N., and BROOK, D.L. Phys. Fluids, 12, 347, 1969.

8. KRALL, N., and BOOK, D.L. Phys. Rev. Lett. 23, 574, 1969 and Private Communication

9. KADOMTSEV, B. Plasma Turbulence, Academic Press, 1965.

10. EVAN, D.E. and KATZENSTEIN, J. Rep. on Prog. in Physics, 32, 207, 1969.

11. BEKEFI, G. Radiation Processes in Plasmas, Wiley, 1966.

12. ROSENBLUTH, M.N., ROSTOCKER, N. Phys. Fluids 5, 776, 1962.

13. PAUL, J.W.M., DAUGHNEY, C.C., and HOLMES, L.S. Inst. Phys. and Phys. Soc. (London) Conference on Plasma Diagnostics, Culham, 1968 (Reviewed Nature 218, 324, 1968) and A.P.S. Conference on Plasma Instabilities in Astrophysics Asilomar, October, 1968.

14. PAUL, J.W.M., DAUGHNEY, C.C., and HOLMES, L.S., Nature 223, 822, 1969.

15. RUDDER, R.R. and BACK, D.R. J. Opt. Soc.Amer., 58, 1260.

16. DENISSEE, J.F., and DELCROIX, J.L. Plasma Waves, Interscience, 1963.

17. MOORCROFT, D.R. J. Geophys. Res. 68, 4870, 1963.

18. SITENKO, A.G. Electromagnetic Fluctuations in Plasmas, 1967, Academic Press.

19. COOK, I., and BICKERTON, R.J. Private discussions

20. THOMPSON, W.B. and HUBBARD, J. Rev. Mod. Phys., 32, 714, 1960.

21. STURROCK, P.A. Phys. Rev. 141, 186, 1966.

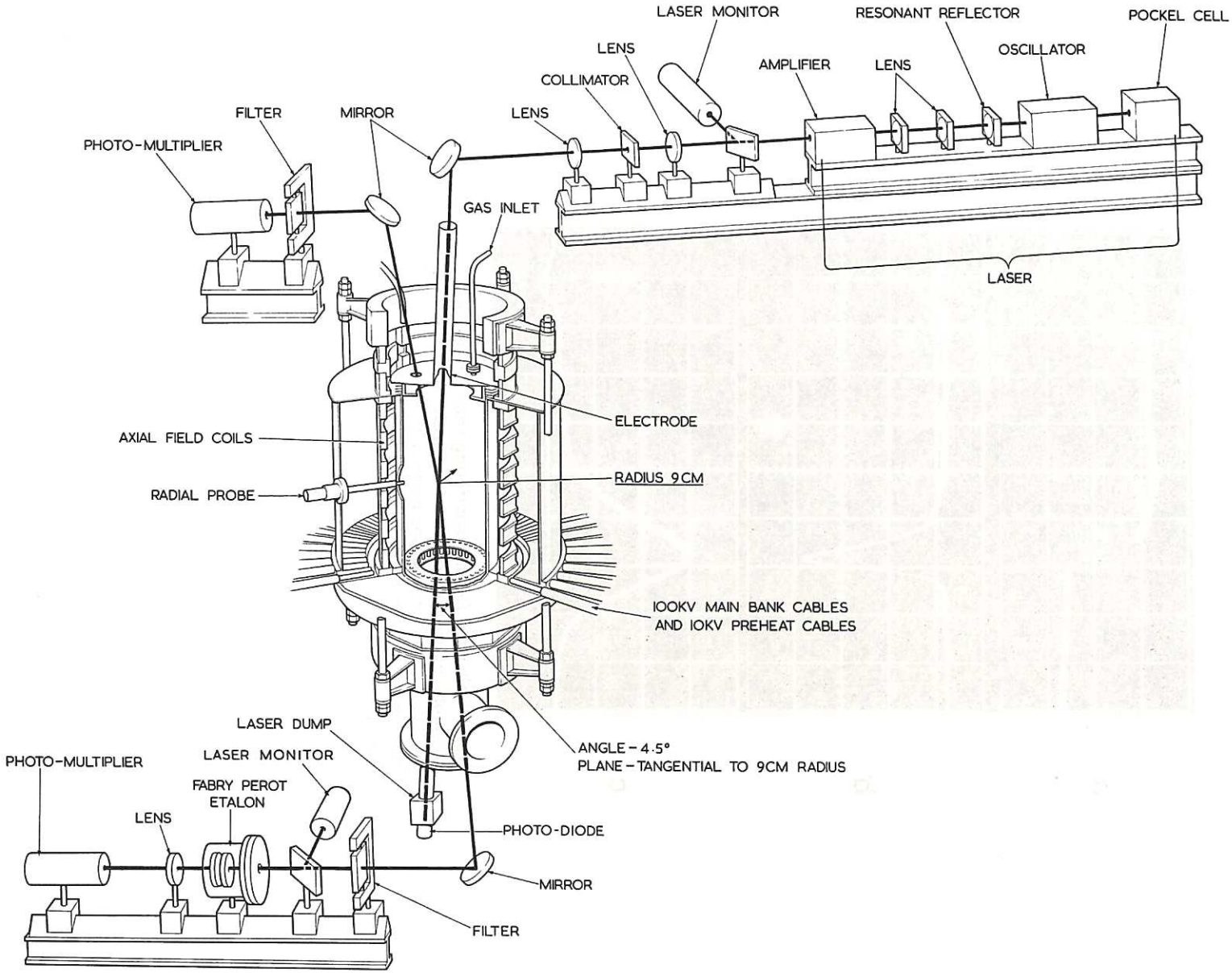

Fig. 1 Experimental arrangement for simultaneous forward and backward scattering measurements on the Tarantula experiment (3)

CLM - P222

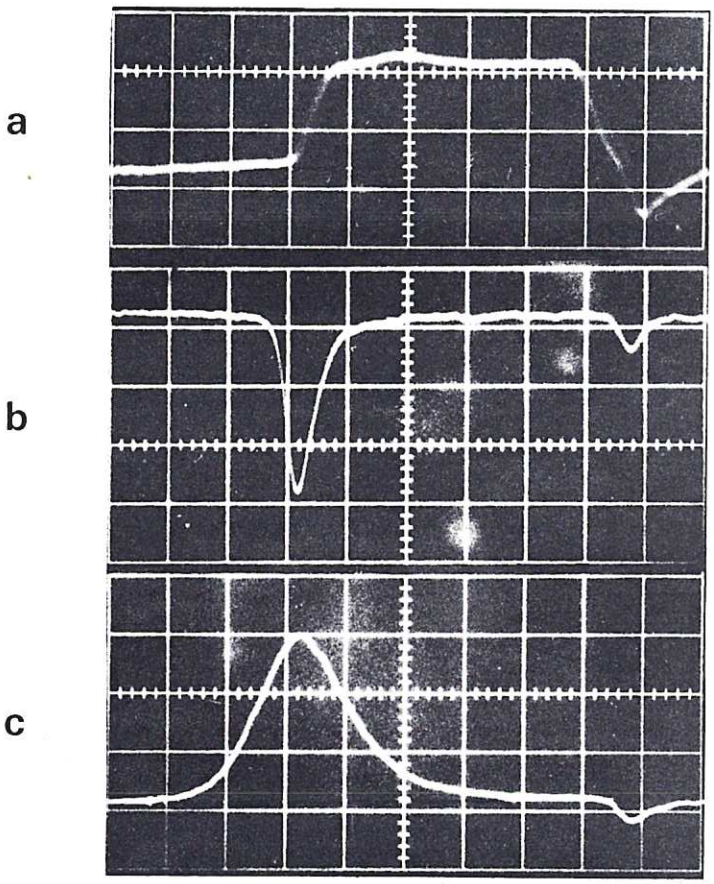

Fig. 2 Enhanced forward scattering from the shock[14] Synchronized records of one event with 20 ns per large division. (a) Electric probe monitor of the shock (b) Forward scattered power with 3 Å filters, (c) Incident laser power

CLM - P 222

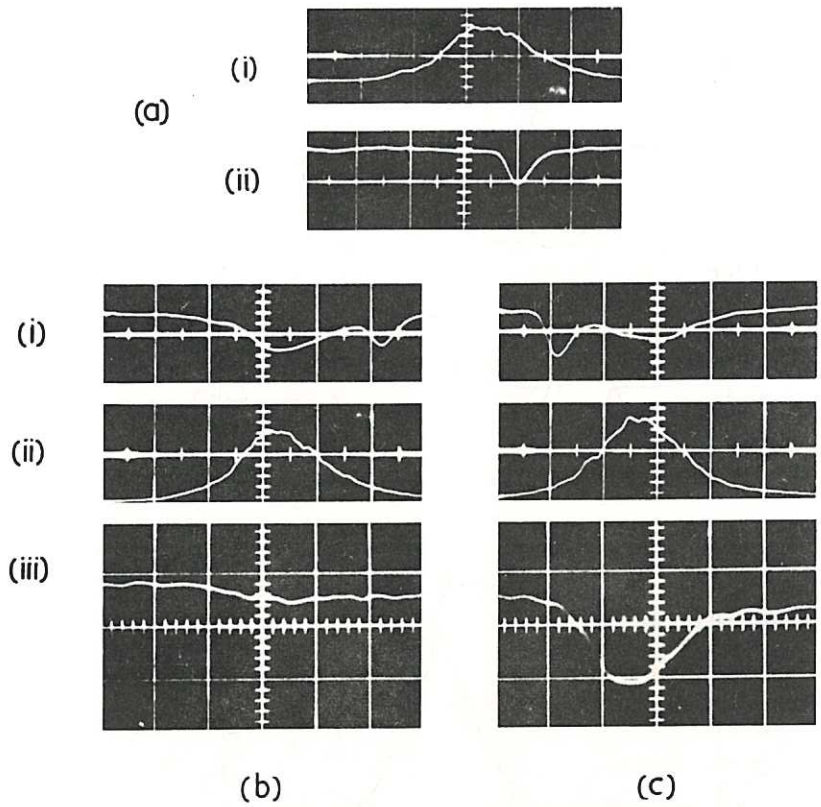

Fig. 3 Enhanced forward scattering from the shock [3] (20 ns per large division); (a) Shock central on laser pulse, i.Laser power, ii.Forward scattered power; (b) and (c) shock late and early in laser pulse, i.Forward scattered power, ii.Laser power, iii.Backward scattered power.

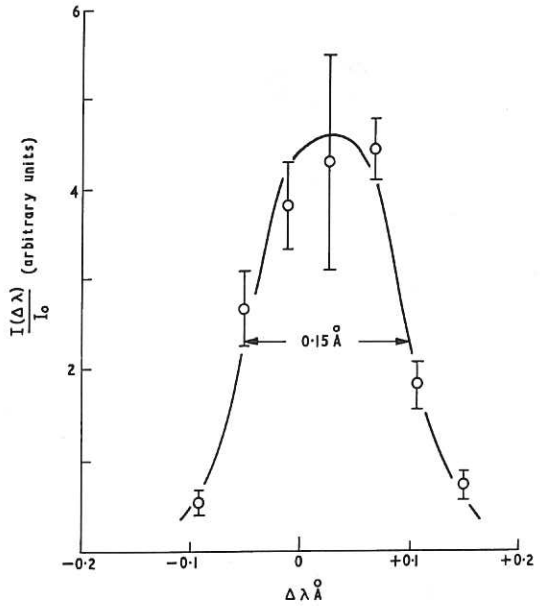

Fig. 4 Spectral profile of forward scattered light from the shock with 0.08 Å resolution [14]. Spurious background of 6% automatically subtracted by pulsed nature of the signal.

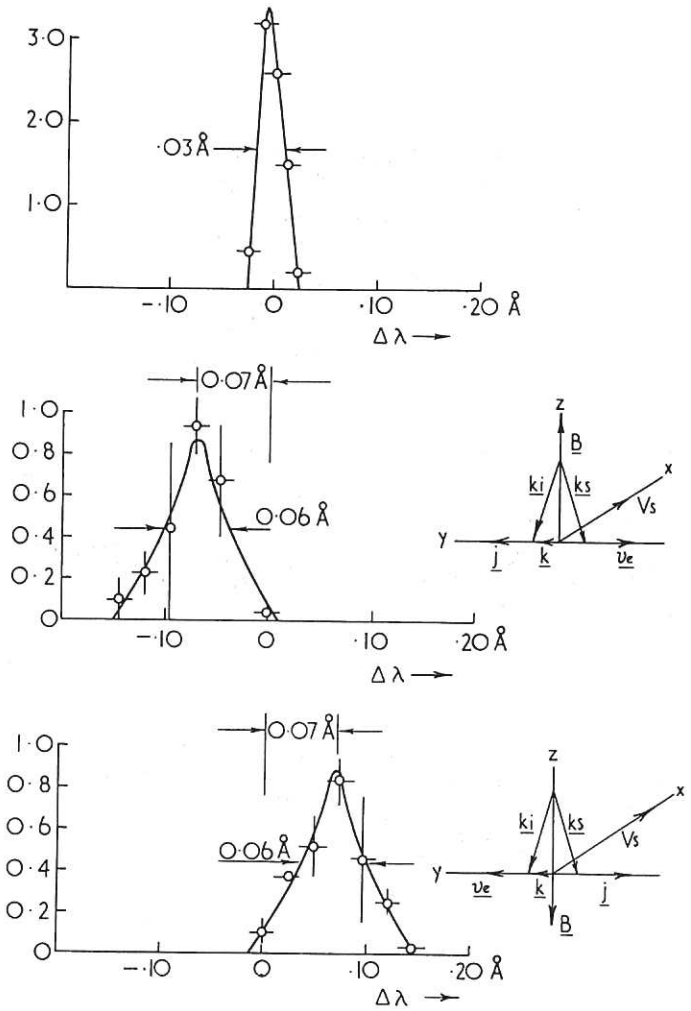

Fig. 5 Spectral profile of incident and forward scattered light with 0.02 Å resolution. (a) Incident laser line, (b) and (c) Profile of light scattered from shock with B_{zl} up and down respectively.

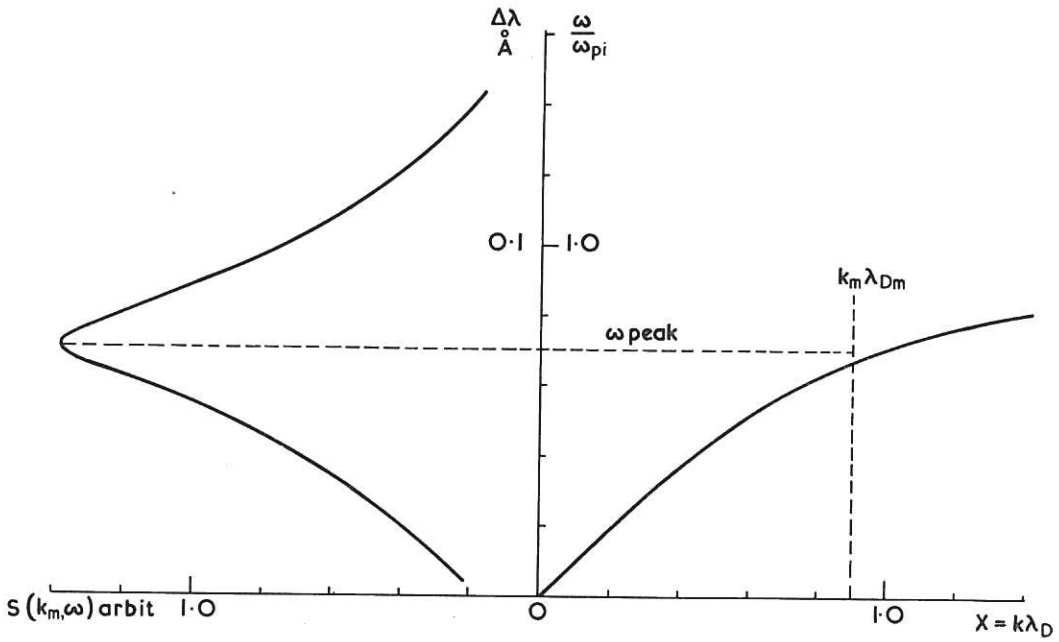

Fig. 6 Measured density fluctuation spectrum $S(\omega, k_m)$ and the simple theoretical ion wave dispersion curve for isothermal electrons with $T_e \gg T_i$.